MITSUBISHI ELECTRIC RESEARCH LABORATORIES
http://www.merl.com

Reduced-Complexity Transmit/Receive-Diversity Systems

Win, M.; Winters, J.

TR2003-44 August 2003

Abstract

We consider wireless systems with transmit and receive diversity. For reduction of complexity, we propose to use hybrid selection/maximal ratio transmission at one link end, choosing L out of N antennas. We analyze the performance of such systems, giving analytical bounds and comparing them to computer simulations. Outage probability, symbol error probability, and capacity are shown. We demonstrate that in typical cases, a small number of used antennas L is sufficient to achieve considerable performance gains. We also analyze the infuence of the number of base station antennas, of fading correlation and channel estimation errors. The simulation results confirm that the proposed scheme is effective in a variety of environments.

Publication History:

1. First printing, TR-2003-44, August 2003

Reduced-Complexity Transmit/Receive-Diversity Systems

Andreas F. Molisch, *Senior Member, IEEE*, Moe Z. Win, *Senior Member, IEEE*,

and Jack H. Winters, *Fellow, IEEE*

The authors were with AT&T Labs - Research, Middletown, NJ. A. F. Molisch is now with MERL Mitsubishi Electric Research Lab, Murray Hill, NJ, and the Department of Electroscience, Lund University, Sweden; email Andreas.Molisch@ieee.org. M. Z. Win is with the Massachusets Institute of Technology, Cambridge, MA, email win@ieee.org. J. H. Winters is with Jack Winters Communications LLC, NJ; email jack@jackwinters.com

Abstract

We consider wireless systems with transmit and receive diversity. For reduction of complexity, we propose to use hybrid selection/maximal ratio transmission at one link end, choosing L out of N antennas. We analyze the performance of such systems, giving analytical bounds and comparing them to computer simulations. Outage probability, symbol error probability, and capacity are shown. We demonstrate that in typical cases, a small number of used antennas L is sufficient to achieve considerable performance gains. We also analyze the influence of the number of base station antennas, of fading correlation and channel estimation errors. The simulation results confirm that the proposed scheme is effective in a variety of environments.

Index Terms

Diversity, MIMO, antenna selection, channel estimation

I. Introduction

Systems with multiple antennas at both transmitter and receiver have received considerable attention in recent years [1], [2]. One approach to utilize multiple transmit antennas is to transmit different data streams from each antenna; these streams can be separated at the receiver side by using signal processing techniques such as the so-called BLAST schemes [3], [4]. However, this approach cannot be used with existing standards, as the requirement of backward-compatibility is not fulfilled.

An alternative way for exploiting multiple antenna elements at transmitter and receiver is the use of transmit and receive diversity purely for link-quality improvement, exploiting the diversity effect. Transmit diversity schemes were first proposed in [5], [6] for the enhancement of transmission quality in mobile radio systems. In such a system, the signals supplied to the different transmit antennas are weighted replicas of a single bit stream (which might be coded or uncoded). The ideal weights can be determined by matching them to the channel, resulting in maximal-ratio transmission (MRT) [7]. Similarly, at the receiver, ”standard” maximal-ratio combiningMRC) can be employed, using linear combinations of the signals obtained at the different receive antennas. It has been shown that with N_t transmit and N_r receive antennas, a diversity degree of $N_\text{t}N_\text{r}$ can be achieved [8]. Since it employs no special type of coding, any standard (single-antenna) receiver can detect the transmitted signal (albeit with a smaller diversity degree and thus reduced quality).

The main disadvantage of MRT (MRC) is the fact that it requires N_t (N_r) complete RF chains. There are numerous situations where this high degree of hardware complexity is undesirable - this is especially important for the mobile station (MS). On the other hand, a simple (1 out of N) selection diversity gives considerably worse results. A compromise between these two possibilities is hybrid selection/maximum-ratio combining (H-S/MRC[1] [9], [10], [11], [12], [13]) where the best L out of N antennas are selected, and then combined, thus reducing the number of required RF chains to L.[2]

In this paper, we consider a transmit/receive diversity system where the transmitter uses hybrid selection/maximal-ratio transmission (H-S/MRT), while the receiver uses MRC. We will analyze the performance of such a system in terms of signal-to-noise ratio (SNR), symbol error probability (SEP), and capacity. In Sec. II, we describe the model for the system and the wireless channel. Next, we derive bounds for the system performance in terms of SNR, capacity, and (uncoded) bit error probability. For these theoretical considerations, we use some idealizations. In the next section, we present results both from the theoretical analysis and from Monte Carlo simulations. Those simulations are used to show the validity of our theory, as well as for

[1] H-S/MRC in the following can denote either the transmission or the reception case.

[2] The case that one link end uses MRC, while the other uses pure selection combining, i.e., selecting only a single antenna out of N available, is treated in [14].

investigating the influence of nonidealities in the system. A summary wraps up the paper.

II. System and channel model

Figure 1 shows the generic system that we are considering. A bit stream is sent through an encoder, and a modulator. A multiplexer switches the modulated signals to the best L_t out of N_t available antenna branches. For each selected branch, the signal is multiplied by a complex coefficient u whose actual value depends on the current channel realization. In a real system, the signals are subsequently upconverted to passband, amplified by a power amplifier, and filtered. For our model, we omit these stages, as well as their corresponding stages at the receiver, and treat the whole problem in equivalent baseband. Note, however, that exactly these stages are the most expensive and make the use of reduced-complexity systems desirable.

Next, the signal is sent over a quasi-static flat-fading channel. We denote the $N_\mathrm{r} \times N_\mathrm{t}$ matrix of the channel as H. The output of the channel is polluted by additive white Gaussian noise, which is assumed to be independent at all receiver antenna elements. The received signals are multiplied by complex weights w^* at all antenna elements (where superscript * denotes complex conjugation), and combined before passing a decoder/detector.

For the theoretical analysis in Sec. III, we make some additional simplifying assumptions:

(i) The fading at the different antenna elements is assumed to be independent, identically distributed Rayleigh fading. The h_{ij} are modeled as independent identically distributed zero-mean, circularly symmetric complex Gaussian random variables with unit variance, i.e. the real and imaginary part each have variance $1/2$. Consequently, the power carried by each transmission channel (h_{ij}) is chi-square distributed with 2 degrees of freedom.Theoretically, also Nakagami fading with integer m-parameter is possible within the framework of our computation method.

However, we note that Nakagami fading with $m > 1$ that is independent at the different antenna elements rarely occurs in practice, as a large Nakagami parameter indicates line-of-sight, which induces correlation between the fading. The influence of correlation on the achievable capacity will be discussed in Sec. IV.

(ii) The fading is assumed to be frequency flat. This is fulfilled if the coherence bandwidth of the channel is significantly larger than the system bandwidth.

(iii) We assume that both transmitter and receiver have perfect knowledge of the channel. This is, of course, an idealization that can only be approximated even in slowly fading channels. The receiver can obtain its channel knowledge either from the demodulation of training sequences (in TDMA systems) or pilot tones (for CDMA or OFDM systems). Alternatively, the use of blind channel estimation methods is a viable approach but results in a higher complexity. The transmitter can obtain the channel information either by feedback from the receiver, or from the antenna weights generated on reception at the transmitter on the reverse link. Note that the latter approach requires the duplex frequency separation to be much smaller than the coherence bandwidth (in a frequency division duplexing scheme) or the duplex time to be much smaller than the coherence time of the channel (in a time-division duplexing scheme). In practical systems, the former condition is usually violated, while the latter condition is fulfilled. Especially, cordless systems like DECT (Digital Enhanced Cordless Telecommunications) [15], PHS (Personal Handyphone System) [16], or PACS [17] exhibit duplex times of a few milliseconds, which are considerably less than the typical coherence time, which is related to the inverse of the maximum Doppler frequency at pedestrian movement speeds. The influence of wrong antenna selection due to channel estimation errors will be discussed in Sec. IV.

III. Computation of performance

A. Channel statistics and optimum weights

We first have to determine the optimum antenna weights, and the statistics of the fading channel. The easiest way for deriving the optimum weights is a singular value decomposition of the channel matrix $H = U\Lambda W^*$, where Λ is a diagonal matrix containing the singular values, and U and W^* are unitary matrices composed of the left and right singular vectors, respectively [18]. The optimum transmit weight vector $\overrightarrow{u}$ and optimum receive weight vector $\overrightarrow{w^*}$, respectively, can now be shown to be the left and right singular vectors belonging to the largest singular value [8]. The effective SNR is given by the square of this singular value, i.e. the eigenvalue of $HH^\dagger$, where superscript † denotes Hermitian transpose. Note that this derivation assumes the use of all available antennas at both transmitters and receivers.

Our goal here is to determine the performance when only a subset of the antennas are used. For this, we have to define a set of matrices $\widetilde{H}$, where $\widetilde{H}$ is created by striking $N_\mathrm{t} - L_\mathrm{t}$ columns from H, and $S(\widetilde{H})$ denotes the set of all possible $\widetilde{H}$, whose cardinality is $\binom{N_\mathrm{t}}{L_\mathrm{t}}$. The achievable SNR of the reduced-complexity system is now

$$\gamma_{\mathrm{H-S/MRC}} = \max_{S(\widetilde{H})} \left(\max_i (\widetilde{\lambda}_i^2) \right) \tag{1}$$

where the $\widetilde{\lambda}_i$ are the singular values of $\widetilde{H}$.

An analytical solution $SNR_{\mathrm{H-S/MRC}}$ does not seem to be easily obtainable. However, we can derive upper and lower bounds. We start out by stating that

$$\frac{1}{\min(L_\mathrm{t}, N_\mathrm{r})} \sum_i \widetilde{\lambda}_i^2 \leq \max_i (\widetilde{\lambda}_i^2) \leq \sum_i \widetilde{\lambda}_i^2 \tag{2}$$

i.e., the achievable SNR for a certain modified channel matrix $\widetilde{H}$ is lower-bounded by the *average* of the nonzero eigenvalues, and upper-bounded by the *sum* of the nonzero eigenvalues of

$\widetilde{H}$. We thus can bound the SNR of the selective-transmit - receive diversity system by finding

$$\gamma_{\mathrm{bound}} = \max_{S(\widetilde{H})} \left(\sum_i \widetilde{\lambda}_i^2 \right) = \max_{S(\widetilde{H})} \left(\sum_i \sum_j |\widetilde{h}_{ij}|^2 \right) \tag{3}$$

We note here also that the antenna combination that gives the maximum $\sum_i \widetilde{\lambda}_i^2$ is not necessarily the antenna combination that gives the maximum $\max_i(\widetilde{\lambda}_i^2)$.[3] However, the bounds of (2) remain valid when the maximization over all antenna combinations is applied to them.

Now the maximization in (3) can also be interpreted as being performed over various combinations of L_{t} out of N_{t} columns, while the rows of the matrix always have dimension N_{r}. Thus, $\gamma_i = \sum_{j=1}^{N_{\mathrm{r}}} |\widetilde{h}_{ji}|^2$ are (henceforth normalized) chi-square distributed random variables with $2N_{\mathrm{r}}$ degrees of freedom. Note that the γ_i can be interpreted as the received SNR when only the $i-$th antenna is transmitting, and the receiver uses MRC. The joint statistics of the *ordered* SNRs $\gamma_{(i)}$ can be shown to be [11]

$$p_{\gamma_{(i)}}(\gamma_{(1)}, \gamma_{(2)}, \dots \gamma_{(N_{\mathrm{t}})}) = \begin{cases} N_{\mathrm{t}}! \prod_{i=1}^{N_{\mathrm{t}}} \frac{1}{\Gamma(N_{\mathrm{r}})} \gamma_{(i)}^{N_{\mathrm{r}}-1} \exp\left(-\gamma_{(i)}\right) & \text{for} \quad \gamma_{(1)} > \gamma_{(2)} > \dots > \gamma_{(N_{\mathrm{t}})} \\ 0 & \text{otherwise} \end{cases} . \tag{4}$$

We utilize L_{t} out of N_{t} variables $\gamma_{(i)}$, and choose the combination that gives maximum SNR. The desired γ_{bound} can be easily written in terms of the ordered SNRs as

$$\gamma_{\mathrm{bound}} = \sum_{i=1}^{L_{\mathrm{t}}} \gamma_{(i)} \tag{5}$$

B. Statistics of the SNR

The statistics of γ_{bound} can be derived from (4) and (5). Mathematically, this problem is equivalent to computing the SNR for H-S/MRT with a single receive antenna, but with Nakagami

[3]The practical implications of this statement for antenna selection algorithms will be discussed in Sec. IV.

channel statistics.[4] Consequently, the simple and elegant techniques for analyzing H-S/MRC with single-transmit-antenna in Rayleigh fading channels [19] cannot be used anymore. On the other hand, the available techniques for H-S/MRC in Nakagami-fading [12], [20], while mathematically elegant, do not lend themselves easily to computer implementation. We are thus using a new approach, that also exploits the fact that in our case, the degrees of freedom (i.e. the number of antenna elements) can only take on integer values.

Since we are computing the sum of random variables, computing the characteristic function suggests itself naturally. We can write it as

$$\Phi(j\nu) = \frac{N_{\mathrm{t}}!}{\Gamma(N_{\mathrm{r}})^{N_{\mathrm{t}}}} \int_0^\infty d\gamma_{(1)} \gamma_{(1)}^{N_{\mathrm{r}}-1} e^{-\gamma_{(1)}} e^{-j\nu\Xi(L_{\mathrm{t}}-1)\gamma_{(1)}} \int_0^{\gamma_{(1)}} d\gamma_{(2)} \gamma_{(2)}^{N_{\mathrm{r}}-1} e^{-\gamma_{(2)}} e^{-j\nu\Xi(L_{\mathrm{t}}-2)\gamma_{(2)}} \ldots \int_0^{\gamma_{(N_{\mathrm{t}}-1)}} d\gamma_{(N_{\mathrm{t}})} \gamma_{(N_{\mathrm{t}})}^{N_{\mathrm{r}}-1} e^{-\gamma_{(N_{\mathrm{t}})}} e^{-j\nu\Xi(L_{\mathrm{t}}-N_{\mathrm{t}})\gamma_{(N_{\mathrm{t}})}} \tag{6}$$

where $\Xi(x)$ is the Heaviside step function

$$\Xi(x) = \begin{cases} 1 & \text{if} \quad x \geq 0 \\ 0 & \text{otherwise} \end{cases} . \tag{7}$$

In the following, we abbreviate the expression $1 - j\nu\Xi(L_{\mathrm{t}} - i)$ as a_i, dropping the dependence on ν for notational convenience. This multiple integral can be shown to result in a polynomial, whose coefficients can be derived analytically by a finite recursion with N_{t} iteration steps.

The crucial step of our proposed technique is now to recognize that an expression of the form

$$\left(d + \sum_p \exp(-b_p x) \wp(p, x) \right) \tag{8}$$

[4]Note that the normalization in a Nakagami channel is usually different from the one used when MRC-combining several Rayleigh-fading channels. However, that is a detail that does not influence the mathematical approach to computing the distribution.

where $\wp(p,x)$ is a polynomial in x whose coefficients may depend on p, retains its basic structure when integrated between 0 and y. Thus, the first $N_{\mathrm{t}}-1$ integrations can be written in an iterative fashion.

Specifically, let us write the integrand for the first integration (i.e. $q=0$) as

$$\gamma_{(N_{\mathrm{t}})}^{N_{\mathrm{r}}-1} \exp\left(-\gamma_{(N_{\mathrm{t}})}\right) I^{(0)} \tag{9}$$

and quite generally denote the result of the qth integration as $I^{(q)}$, where superscript $^{(q)}$ indexes the number of performed integrations. The integral $I^{(q)}$ has the form

$$I^{(q)} = d^{(q)} + \sum_{p=1}^{q} e^{-b_p^{(q)}\gamma_{(N_{\mathrm{t}}-q)}} \sum_{k=0}^{(q-p+1)(N_{\mathrm{r}}-1)} c_{p,k}^{(q)} \gamma_{(N_{\mathrm{t}}-q)}^{k} \tag{10}$$

with initial condition

$$d^{(0)} = 1 \quad b_p^{(0)} = 0 \quad c_{p,k}^{(0)} = 0 \ . \tag{11}$$

We show in the appendix that the central quantities $d^{(q)}, b_p^{(q)}$, and $c_{p,k}^{(q)}$ are given by recursion relations

$$b_p^{(q+1)} = b_p^{(q)} + a_{N_{\mathrm{t}}-q} \qquad \text{for} \qquad 1 \le p \le q; \tag{12}$$

$$b_{q+1}^{(q+1)} = a_{N_{\mathrm{t}}-q} \tag{13}$$

$$\widehat{c}_{p,k}^{(q)} = \begin{cases} c_{p,k-(N_{\mathrm{r}}-1)}^{(q)} & \text{for} \quad (q-p+2)(N_{\mathrm{r}}-1) \ge k \ge (N_{\mathrm{r}}-1) \\ 0 & \text{otherwise} \end{cases} \tag{14}$$

$$d^{(q+1)} = d^{(q)} \frac{(N_{\mathrm{r}}-1)!}{(a_{N_{\mathrm{t}}-q})^{N_{\mathrm{r}}}} + \sum_{p=1}^{q} \sum_{t=0}^{(q-p+2)(N_{\mathrm{r}}-1)} \frac{t!\,\widehat{c}_{p,t}^{(q)}}{(b_p^{(q+1)})^{t+1}} \tag{15}$$

$$c_{p,k}^{(q+1)} = -\sum_{t=0}^{(q-p+2)(N_{\mathrm{r}}-1)-k} \frac{\widehat{c}_{p,k+t}^{(q)}}{(b_p^{(q+1)})^{t+1}} \frac{(k+t)!}{k!} \tag{16}$$

for $1 \leq p \leq q$ and

$$c_{p,k}^{(q+1)} = -\frac{d^{(q)}}{(b_p^{(q+1)})^{N_\mathrm{r}-k}} \frac{(N_\mathrm{r}-1)!}{k!} \tag{17}$$

for $p = q+1$.

The characteristic function of the γ_{bound} is finally given as

$$\Phi(j\nu) = \frac{N_\mathrm{t}!}{\Gamma(N_\mathrm{r})^{N_\mathrm{t}}} \Big[d^{(N_\mathrm{t}-1)}(N_\mathrm{r}-1)! a_1^{-N_\mathrm{r}} + \sum_{p=1}^{N_\mathrm{t}-1} \sum_{t=0}^{(N_\mathrm{t}-p+1)(N_\mathrm{r}-1)} \widehat{c}_{p,t}^{(N_\mathrm{t}-1)} t! (b_p^{(N_\mathrm{t})})^{-(t+1)} \Big] . \tag{18}$$

Note that this is the characteristic function $\Phi(j\nu)$, where the coefficients $d^{(N_\mathrm{t})}$, $\widehat{c}_{p,t}^{(N_\mathrm{r})}$, and $b_p^{(N_\mathrm{t})}$ depend on $j\nu$.

In principle, an analytic inversion of the characteristic function would be possible, giving the probability density function of the SNR $p_{\gamma_{\mathrm{bound}}}(\cdot)$ in closed form. However, due to the existence of fast Fourier inversion techniques [21], numerical inversion is convenient and fast.

C. Bit Error Probability

Computation of the bit error probability (BEP) can be done by the classical method of averaging the ”instantaneous BEP” (i.e. BEP for one given channel realization) over the statistics of the SNR. For coherent demodulation, this gives

$$P_e = K \int_0^\infty Q(\sqrt{a\gamma_{tot}}) p_{\gamma_{tot}}(\gamma_{tot}) d\gamma_{tot} \tag{19}$$

where$Q$ is the Gaussian Q-function as defined in [22], and the constants K and a depend on the modulation format [22].

However, since we are computing the characteristic function anyway, it seems preferable to do the computations in that domain. Minimum shift keying with precoded transmitter and derotation of the signal constellation diagram [23] exhibits the same error probability as BPSK. Thus, the error probability can be computed as [24], [25]

$$P_e = \int_0^{\pi/2} \Phi\left(j\frac{1}{\sin^2(\phi)}\right) d\phi \tag{20}$$

For $\pi/4$-shifted DQPSK (with Gray coding and differential detection), we obtain [26]

$$P_e = \frac{1}{4\pi}\int_{-\pi}^{\pi} \frac{1-\zeta^2}{1+2\zeta\sin(\phi)+\zeta^2}\Phi\left(j\frac{2+\sqrt{2}}{2}(1+2\zeta\sin(\phi)+\zeta^2)\right) d\phi \tag{21}$$

where

$$\zeta = \sqrt{\frac{2-\sqrt{2}}{2+\sqrt{2}}}\,. \tag{22}$$

D. Capacity

For a capacity point of view, the whole system between encoder and decoder can be viewed as an effective scalar flat fading channel that is characterized by the SNR $\gamma_{\mathrm{H-S/MRC}}$ as defined in (1). The capacity for each channel realization is thus given by

$$C(\gamma_{\mathrm{H-S/MRC}}) = \log_2(1+\overline{\Gamma}\gamma_{\mathrm{H-S/MRC}}). \tag{23}$$

where $\overline{\Gamma}$ is the average SNR of a SISO (single-input single-output) channel. An upper bound for the capacity is obtained by substituting γ_{bound}, as computed in Sec. III.B, for $\gamma_{\mathrm{H-S/MRC}}$ (and similarily for the lower bound). Using standard techniques for functions of one random variable [27], the upper bound for the pdf of the capacity becomes

$$p_C(C) = 2^C\frac{\ln(2)}{\overline{\Gamma}}p_{\gamma_{\mathrm{bound}}}\left(\frac{(2^C-1)}{\overline{\Gamma}}\right). \tag{24}$$

E. Monte Carlo (MC) simulations

For the influence of nonidealities, we have to take refuge to computer simulations. We first generate one realization of a multiple transmit/receive antenna channel transfer matrix. For the i.i.d, distributed case, this is trivial, as the entries are by definition just independent complex Gaussian random variables. Correlated entries can be created by multiplying the i.i.d. matrix with a matrix $\underline{A}$ that fulfills $\underline{AA}^H = \underline{R}$, where $\underline{R}$ is the desired correlation matrix. We then create submatrices of size $N_\mathrm{r} \times L_\mathrm{t}$, by striking $(N_\mathrm{t} - L_\mathrm{t})$ columns from the channel matrix. For each submatrix, we compute the signal-to-noise ratio SNR (corresponding to the square of the largest singular value). Finally, we select the antenna combination (submatrix) that gives the largest SNR, and store it. This procedure is repeated N_MC times to give a statistical ensemble.

IV. Results

In this section, we present results from our computations and discuss the influence of the number of available, and actually chosen, antennas on the system performance. Unless otherwise stated, we will use the following system parameters: $\overline{\Gamma} = 20$ dB, $N_\mathrm{r} = 2$. $N_\mathrm{t} = 8$. For the BEP computations, we use minimum shift keying $\pi/4-$DQPSK or MSK since these are commonly used in mobile radio systems.

A. Results in idealized environments

Figure 2 shows the cumulative distribution of the capacity for different values of L_t (as obtained from Monte Carlo simulations). We see that the capacity obtained with $L_\mathrm{t} = 3$ is already very close to the capacity of a full-complexity scheme. We also see that the improvement by going from one to three antennas is larger than the gain going from three to eight. For comparison, we also show the capacity with pure MRT. The required number of RF chains is L_t for the H-S/MRT case and N_t for the pure MRT case. Naturally, the capacity is the same for H-S/MRT with $L_\mathrm{t} = 8$, and MRT with $N_\mathrm{t} = 8$. For a smaller number of RF chains, however, the hybrid scheme is much more effective (for the same number of RF chains), both in terms of diversity degree (slope of the curve) and ergodic capacity. This confirms the effectiveness of using H-S/MRT.

Figure 3 shows the cumulative distribution function (cdf) of the capacity for different numbers of selected antennas, $L_{\rm t}$. The exact curve was computed by MC simulations, the upper and lower bounds were computed by the analytical method described in Sec. 3. We note that upper and lower bound are 1 bit/s/Hz apart, except for the case $L_{\rm t} = 1$, where they coincide and agree with the exact curve.

Apart from the bounds and the exact curves (computed by MC simulations), we also exhibit the cdf of the capacity when a suboptimum antenna selection criterion is used. This criterion works the following way: we transmit from a single antenna, $i = 1$, and determine the SNR that can be obtained at the receiver with MRC. Then, we transmit from the next antenna, $i = 2$, and determine again the SNR with MRC, and so on. Then, the $L_{\rm t}$ antennas that resulted in the best SNR are chosen. This can also be interpreted as optimizing $\gamma_{\rm bound}$ instead of $\lambda_{\rm max}$. The advantage of this technique is that the determination of the ”optimum” antennas is much simpler than if we have to make a full search among all possible antenna combinations. Furthermore, the loss in performance is less than 0.05 bits/s/Hz. Note that an alternative antenna selection scheme, based on eigenprecoding, was proposed in [28].

Figure 4 shows the increase of the ergodic capacity and 5% outage capacity as a function of the number of selected antennas. We see that increasing that number from 1 to 2 gives about the same gain as increasing from 2 to 8. It seems thus reasonable to use only 2 or 3 selected antennas, resulting in large cost savings with only a small performance loss.

Figure 5 shows the downlink BEP of $\pi/4-$DQPSK as a function of the mean SNR $\overline{\Gamma}$ for different number of selected antennas $L_{\rm t}$. Again, we observe a big improvement going from

$L_\text{t} = 1$ to $L_\text{t} = 3$ (3 dB at a error probability $P_e = 10^{-3}$), while the gain going from $L_\text{t} = 3$ to $L_\text{t} = 8$ is only an additional 1.5 dB.

Generally, the achieved capacities are much lower than those usually associated with multiple-input - multiple-output (MIMO) systems. The difference is due to the restriction of the possible structures of the transmitter and receiver, allowing for only a single data stream to be transmitted. Specifically, we allow only a scalar coder, and distinguish the signals at the different antennas only by linear weights, not by different codes at each antenna. Comparisons with MIMO systems show that with appropriate (space-time) processing and coding, an outage capacity of 16 bits/s/Hz is possible for $L_\text{t} = 8$, $N_\text{r} = 2$ [29]. The difference with the 10 bits/s/Hz obtained with the linear system is the price for backward compatibility and greater simplicity. We also note that the increase in capacity slows down as we increase L_t, but shows no sharp discontinuity as L_t increases beyond $N_\text{r} = 2$. This is due to the fact that we use linear transmitters and receivers, so that every gain in SNR readily translates into a gain in capacity.

B. Effect of nonidealities

Figure 6 shows the influence of correlation between the transmit antenna elements on the performance of the hybrid system. We show the 10% outage capacity of a $3/8$ system (i.e., $L_\text{t} = 3$, $N_\text{t} = 8$, with 2 receive antennas) for (i) optimum selection of the transmit antennas (i.e., choosing the transmit antennas that give the best SNR), (ii) with power-controlled selection of the transmit antennas as desribed above, and (iii) with MRT with $N_\text{t} = 8$. The outage capacity is plotted as a function of the ratio of correlation length of the channel to antenna spacing. We observe that the relative performance loss due to correlation is higher for the $3/8$ system than for the $8/8$ system. This can be explained by the fact that in a highly correlated channel, no diversity gain can be achieved, but all gain is due to beamforming. Thus antenna selection is ineffective, and the (beamforming) gain is only influenced by the number of actually used antenna elements. We furthermore observe that the difference between the SNR-based criterion for the antenna selection and the optimum antenna selection decreases as the correlation between the antennas increases, and vanishes at very large correlations. This makes sense, as the difference between the chosen antenna signals vanishes for highly correlated signals.

Figure 7 shows the influence of the number of antenna elements at the receiver. We find that as the number of receive antennas increases, the advantage of going from a 1/8 to a 8/8 system at the transmitter decreases. This is intuitively clear, as the beneficial effect of adding diversity antennas is smaller if there are already a lot of diversity antennas.

We have also investigated the influence of erroneous antenna selection on the capacity of the system. We assume that in a first stage, the complete channel transfer matrix is estimated. Based on that measurement, the antennas that are used for the actual data transmission are selected, and the antenna weights are determined. We distinguish four different cases: (i) perfect choice of the antennas and the antenna weights, (ii) imperfect antenna selection, but perfect antenna weights (this can be achieved by measuring the transfer function of the actually selected antennas with a longer training sequence), (iii) imperfect choice of the antennas, as well as of the antenna weights at the transmitter, and perfect antenna weights at the receiver (this is plausible if the feedback is done with finite precision and a finite lag), and (iv) imperfect choice of the antenna weights at transmitter and receiver. The errors in the transfer functions are assumed to have a complex Gaussian distribution with SNR_{pilot}, which is the SNR during the transmission of the pilot tones. We found that measurement with an SNR_{pilot} of 10 dB results in a still tolerable loss of capacity (less than 5%). However, below that level, the capacity starts to decrease significantly. This is shown in Figure 8.

V. RESULTS IN MEASURED CHANNELS

We have also investigated the performance of our proposed scheme in measured channels. The measurements took place in a microcellular environment, specifically in a courtyard in Ilmenau, Germany. Four different measurement scenarios have been analyzed, and full details of the measurement scenarios can be found in [30]. For clarity only two scenarios are presented here, and they are[5]:

Scenario I: Closed back-yard of size $34m \times 40m$ with inclined rectangular extension. The receiver array is situated in one rectangular corner with the array broad side pointing under 45^o inclination directly to the middle of the back-yard. The LOS connection between the transmitter and the receiver is $28m$.

Scenario II: Same back-yard as in scenario I, but with artificially obstructed LOS path. It is expected that the metallic objects generate serious multi-path and high order scattering that can only be observed within the dynamic range of the measurement system if the strong LOS path is obstructed.

The main features of the measured channels are that (i) the number of multipath components with significant amplitude is limited. Using high-resolution algorithms, we found between 20 and 40 multipath components; (ii) the angular spectrum of the arriving waves deviates from a uniform spectrum; the angular spread at the receiver is limited by the opening angle of the used antenna to less than 120 degrees; (iii) the LOS component in Scenario I leads to a higher correlation between the signals.

[5] Scenario I and II correspond to scenario II and III in [30], respectively.

In order to determine distributions of channel capacity and eigenvalues, a large number of measurements are required, which means a large effort. Thus, for the measured channels we evaluate the different distributions by a method introduced in [31], in order to keep the number of required measurements to a reasonable number. This method means that the double directional impulse response is measured, i.e. direction of departure, direction of arrival, time delay and power of the different taps. Then several impulse responses are *synthetically* generated from these measurements by assigning independent uniformly distributed $[0, 2\pi]$ random phases, α_k, to the different realizations of $h_{m,n}$ as

$$h_{m,n} = \sum_{k=1}^{K} A_k e^{j\phi_k} e^{-j\frac{2\pi}{\lambda}d\left(m\sin\left(\Omega_{R,k}\right)+n\sin\left(\Omega_{T,k}\right)\right)} e^{j\alpha_k} \tag{25}$$

where m and n index the antenna elements, K is the number of multipath components, A_k and ϕ_k is the magnitude and phase of the $k-th$ multipath component, and $\Omega_{R,k}$ and $\Omega_{T,k}$ is the angle between the multipath component and the receive- and transmit array, respectively. The α_k stay unchanged as the different antenna elements are considered.

Figure 9 shows plots of the capacity for a $3/8$ H-S/MRT system and an 8-element MRT scheme. The number of receive antennas in both cases is $N_{\mathrm{r}} = 2$. We see that the performance that can be achieved in that environment is very close to the performance in i.i.d. channels, and sometimes it is even better.

VI. Summary and conclusions

We have investigated reduced-complexity wireless systems with transmit and receive diversity. The complexity reduction is achieved by using H-S/MRT on one link end, and MRC at the other. We note that for MRT and H-S/MRC, the results are equally applicable. Since the transceiver structure employs only weighted versions of the same signals, such a system is fully compatible with existing mobile radio systems, while the use of multiple antennas at both transmitter and receiver results in a high degree of diversity. The H-S/MRT(C) offers advantages when a large number of transmit antennas is available, but the number of RF chains should be limited. By choosing the best L_t out of N_t antennas, little signal quality is lost compared to the full-complexity version, while drastically reducing the involved hardware expenses. We have seen that for a practically useful example ($N_\mathrm{t} = 8, N_\mathrm{r} = 2$, $SNR = 20$ dB), $L_\mathrm{t} = 2$ to 3 is a good compromise between hardware expense and performance.

In summary, we find that a reduced-complexity multiple transmit/receive antenna system can bring remarkable improvement in the transmission quality of existing systems, while requiring only moderate hardware expenses, and keeping backward compatibility. For a system that is to be designed from scratch, on the other hand, the use of space time coding instead of a linear transceiver structures would offer advantages both from a capacity point of view and from the fact that it can also be easily applied to FDD systems, since channel knowledge at the transmitter is not required.

Acknowledgments: This work was supported financially in part by the Austrian ministry of education and science, TU Wien, and Oesterreichische Forschungsgemeinschaft, and an INGVAR grant of the Swedish Strategic Research foundation.

VII. Appendix: Derivation of the recursion relation

The starting point is (10) combined with Eq. (6)

$$\int_0^y \left[d^{(q)} + \sum_{p=1}^{q} \exp\left(-b_p^{(q)} x\right) \sum_{k=0}^{(q-p+1)(N_\mathrm{r}-1)} c_{p,k}^{(q)} x^k \right] x^{N_\mathrm{r}-1} \exp\left(-x a_{N_\mathrm{t}-q}\right) dx \qquad (26)$$

where for easier readability we have substituted $\gamma_{N_{\mathrm{t}}-q} \to x$, $\gamma_{N_{\mathrm{t}}-q-1} \to y$.

The first term of the integral (26) can be solved as [32]

$$\int_0^y d^{(q)} x^{N_{\mathrm{r}}-1} \exp\left(-x a_{N_{\mathrm{t}}-q}\right) dx = d^{(q)} \left[\frac{1}{a_{N_{\mathrm{t}}-q}^{N_{\mathrm{r}}}} (N_{\mathrm{r}}-1)! - \frac{\exp(-a_{N_{\mathrm{t}}-q} y)}{a_{N_{\mathrm{t}}-q}^{N_{\mathrm{r}}}} \sum_{k=0}^{N_{\mathrm{r}}-1} \frac{(N_{\mathrm{r}}-1)!}{k!} a_{N_{\mathrm{t}}-q}^{k} y^{k} \right] \tag{27}$$

Next, we pull out from the integral sign the summation over p, and consider the p-th term in the integral 26

$$J_q = \int_0^y \left[\exp\left(-b_p^{(q)} x\right) \sum_{k=0}^{(q-p+1)(N_{\mathrm{r}}-1)} c_{p,k}^{(q)} x^k \right] x^{N_{\mathrm{r}}-1} \exp\left(-x a_{N_{\mathrm{t}}-q}\right) dx \tag{28}$$

By introducing

$$\widehat{b_p}^{(q)} = b_p^{(q)} + a_{N_{\mathrm{t}}-q} \text{ for } 1 \leq p \leq q, \tag{29}$$

$$\widehat{b}_{q+1}^{(q)} = a_{N_{\mathrm{t}}-q}, \tag{30}$$

$$M = (q-p+2)(N_{\mathrm{r}}-1) \tag{31}$$

$$\widehat{c}_{p,k}^{(q)} = \begin{cases} c_{p,k-(N_{\mathrm{r}}-1)}^{(q)} & \text{for} \quad (q-p+2)(N_{\mathrm{r}}-1) \geq k \geq (N_{\mathrm{r}}-1) \\ 0 & \text{otherwise} \quad . \end{cases} \tag{32}$$

this integral can be written as

$$\int_0^y \exp\left(-\widehat{b}_p^{(q)} x\right) \sum_{k=0}^{M} \widehat{c}_{p,k}^{(q)} x^k dx \tag{33}$$

Employing [33]

$$\int \sum_{k=0}^{M} \widehat{c}_{p,k}^{(q)} x^k e^{-\widehat{b}_p^{(q)} x} dx = \frac{e^{-\widehat{b}_p^{(q)} x}}{-\widehat{b}_p^{(q)}} \sum_{l=0}^{M} \frac{(-1)^l}{(-\widehat{b}_p^{(q)})^l} \frac{d^l}{dx^l} \sum_{k=0}^{M} \widehat{c}_{p,k}^{(q)} x^k \tag{34}$$

we get

$$\begin{aligned} J_q &= \frac{e^{-\widehat{b}_p^{(q)} x}}{-\widehat{b}_p^{(q)}} \sum_{l=0}^{M} \frac{(-1)^l}{(-\widehat{b}_p^{(q)})^l} \sum_{k=0}^{M} \widehat{c}_{p,k}^{(q)} \frac{d^l}{dx^l} x^k \Bigg|_0^y \\ &= \frac{e^{-\widehat{b}_p^{(q)} x}}{-\widehat{b}_p^{(q)}} \sum_{k=0}^{M} \widehat{c}_{p,k}^{(q)} \sum_{l=0}^{k} \frac{1}{(\widehat{b}_p^{(q)})^l} \frac{k!}{(k-l)!} x^{k-l} \Bigg|_0^y \end{aligned} \tag{35}$$

Introducing $r = k - l$, we can write this as

$$J_q = -\frac{e^{-\widehat{b}_p^{(q)} x}}{\widehat{b}_p^{(q)}} \sum_{r=0}^{M} x^r \sum_{t=0}^{M-r} \widehat{c}_{p,r+t}^{(q)} \frac{1}{(\widehat{b}_p^{(q)})^t} \frac{(r+t)!}{r!} \Bigg|_0^y$$

The total integral thus is

$$d^{(q)} \left[\frac{1}{(\widehat{b}_{q+1}^{(q)})^{N_\mathrm{r}}} (N_\mathrm{r}-1)! - \frac{\exp(-\widehat{b}_{q+1}^{(q)} y)}{(\widehat{b}_{q+1}^{(q)})^{N_\mathrm{r}}} \sum_{k=0}^{N_\mathrm{r}-1} \frac{(N_\mathrm{r}-1)!}{k!} (\widehat{b}_{q+1}^{(q)})^k y^k \right] + \tag{37}$$
$$\sum_{p=1}^{q} \left[\frac{1}{\widehat{b}_p^{(q)}} \sum_{t=0}^{M} \widehat{c}_{p,t}^{(q)} \frac{t!}{(\widehat{b}_p^{(q)})^t} - \frac{e^{-\widehat{b}_p^{(q)} x}}{\widehat{b}_p^{(q)}} \sum_{r=0}^{M} y^r \sum_{t=0}^{M-r} \widehat{c}_{p,r+t}^{(q)} \frac{1}{(\widehat{b}_p^{(q)})^t} \frac{(r+t)!}{r!} \right]$$

Comparing this expression with the generic expression for the result of the $q+1$th integration

$$\left[d^{(q+1)} + \sum_{p=1}^{q+1} \exp\left(-b_p^{(q+1)} y\right) \sum_{k=0}^{(q-p+2)(N_\mathrm{r}-1)} c_{p,k}^{(q+1)} y^k \right] \tag{38}$$

and matching coefficients, we get the recursion relations, (12) - (16) given in Sec. 3.2.

For the last integration, we use the fact that [33]

$$\int_0^\infty x^k \exp(-ax) dx = k! a^{-k-1} \tag{39}$$

so that

$$\int_0^y \left[d^{(q)} + \sum_{p=1}^{q} \exp\left(-b_p^{(q)} x\right) \sum_{k=0}^{(q-p+1)(N_\mathrm{r}-1)} c_{p,k}^{(q)} x^k \right] x^{N_\mathrm{r}-1} \exp\left(-x a_{N_\mathrm{t}-q}\right) dx \tag{40}$$
$$= d^{(N_\mathrm{t}-1)} \frac{(N_\mathrm{r}-1)!}{a_1^{N_\mathrm{r}}} + \sum_{p=1}^{N_\mathrm{t}-1} \left[\sum_{t=0}^{(N_\mathrm{t}-p+1)(N_\mathrm{r}-1)} \widehat{c}_{p,t}^{(N_\mathrm{t}-1)} \frac{t!}{(b_p^{(N_\mathrm{t})})^{t+1}} \right]$$

REFERENCES

[1] J. H. Winters, "On the capacity of radio communications systems with diversity in Rayleigh fading environments," *IEEE J. Selected Areas Comm.*, vol. 5, pp. 871–878, June 1987.

[2] G. J. Foschini and M. J. Gans, "On limits of wireless communications in fading environments when using multiple antennas," *Wireless Personal Comm.*, vol. 6, pp. 311–335, 1998.

[3] G. J. Foschini, "Layered space-time architecture for wireless communication in a fading environment when using multi-element antennas," *Bell Labs Techn. J.*, pp. 41–59, Autumn 1996.

[4] G. J. Foschini, G. D. Golden, R. A. Valenzuela, and P. W. Wolniansky, "Simplified processing for high spectral efficiency wireless communication employing multi-element arrays," *IEEE J. Seceted Areas Comm.*, vol. 17, pp. 1841–1852, 1999.

[5] A. Wittneben, "A new bandwidth efficient transmit antenna modulation diversity scheme for linear digital modulation," in *IEEE International Conference on Communications*, (Geneva), pp. 1630–1634, IEEE, 1993.

[6] J. H. Winters, "The diversity gain of transmit diversity in wireless systems with rayleigh fading," in *IEEE International Conference on Communications*, (Piscataway, N.J.), pp. 1121–1125, IEEE, 1994.

[7] T. K. Y. Lo, "Maximum ratio transmission," in *Proc. IEEE Int. Conf. Comm.*, (Piscataway, N.J.), pp. 1310–1314, IEEE, 1999.

[8] J. B. Andersen, "Antenna arrays in mobile communications: gain, diversity, and channel capacity," *IEEE Antennas Propagation Mag.*, pp. 12–16, April 2000.

[9] N. Kong and L. B. Milstein, "Combined average SNR of a generalized diversity selection combining scheme," in *Proc. IEEE Int. Conf. on Commun.*, vol. 3, pp. 1556–1560, June 1998. Atlanta, GA.

[10] M. Z. Win and J. H. Winters, "Analysis of hybrid selection/maximal-ratio combining of diversity branches with unequal SNR in Rayleigh fading," in *Proc. 49th Annual Int. Veh. Technol. Conf.*, vol. 1, pp. 215–220, May 1999. Houston, TX.

[11] M. Z. Win and J. H. Winters, "Virtual branch analysis of symbol error probability for hybrid selection/maximal-ratio combining in Rayleigh fading," *IEEE Trans. Commun.*, vol. 49, pp. 1926–1934, Nov 2001.

[12] M. S. Alouini and M. K. Simon, "Performance of coherent receivers with hybrid SC/MRC over Nakagami-m fading channels," *IEEE Trans. Vehicular Techn.*, vol. 48, pp. 1155–1164, 1999.

[13] R. K. Mallik and M. Z. Win, "Analysis of hybrid selection/maximal-ratio combining in correlated nakagami fading," *IEEE Trans. Commun.*, pp. 1372–1383, Aug. 2002.

[14] M. Engels, B. Gyselinckx, S. Thoen, and L. V. der Perre, "Performance analysis of combined transmit-SC/receive-MRC," *IEEE Trans. Communications*, vol. 49, pp. 5 –8, 2001.

[15] E. T. S. I. (ETSI), "Radio equipment and systems: European cordless telecommunications standard interface," *DECT Specifications*, vol. part 1–3, p. version 02.01, 1991.

[16] J. Gibson, *The mobile radio handbook*. IEEE Press, 1996.

[17] T. S. Rappaport, *Wireless Communications Principles and Practice*. Piscataway, NJ: IEEE Press, 1996.

[18] R. A. Horn and C. R. Johnson, *Matrix Analysis*. Cambridge Univ. Press, 1985.

[19] M. Z. Win and J. H. Winters, "Analysis of hybrid selection/maximal-ratio combining in Rayleigh fading," *IEEE Trans. Commun.*, vol. 47, pp. 1773–1776, Dec. 1999.

[20] M. S. Alouini and M. K. Simon, "Application of the dirichlet transformation to the performance evaluation of generalized selection bomining over Nakagami-m fading channels," *J. of Communiations and Networks*, vol. 1, pp. 5–13, 1999.

[21] W. H. Press and et al., *Numerical Recipes*. Cambridge University Press, 1996.

[22] J. G. Proakis, *Digital Communications*. New York, McGraw Hill, 3rd ed., 1995.

[23] R. S. (Ed.), *Mobile Communications*. Kluwer, 1992.

[24] C. Tellambura, A. J. Mueller, and V. K. Bhargawa, "Analysis of m-ary phase-shift keying with diversity reception for land-mobile satellite channels," *IEEE Trans. Vehicular Technology*, vol. 46, pp. 910–922, 1997.

[25] M. Z. Win, G. Chrisikos, and N. R. Sollenberger, "Performance of Rake reception in dense multipath channels: Implications of spreading bandwidth and selection diversity order," *IEEE J. Select. Areas Commun.*, 2000. to appear.

[26] M. K. Simon and M.-S. Alouini, "A unified approach to the performance analysis of digital communication over generalized fading channels," *Proc. IEEE*, vol. 86, pp. 1858–1877, Sept. 1998.

[27] A. Papoulis, *Probability, Random Variables, and Stochastic Processes*. Tokyo, McGraw Hill, 1965.

[28] R. Inner and G. Fettweis, "Combined transmitter and receiver optimization for multiple-antenna frequency-selective channels," in *Proc. 5th Int. Symp.Wireless Personal Multimedia Communications*, pp. 412 –416, 2002.

[29] A. F. Molisch, M. Z. Win, and J. H. Winters, "Capacity of MIMO systems with antenna selection," in *IEEE International Conference on Communications*, (Helsinki), pp. 570–574, 2001.

[30] M. Steinbauer, A. F. Molisch, and E. Bonek, "The double-directional radio channel," *IEEE Antennas and Propagation Mag.*, pp. 51–63, August 2001.

[31] A. F. Molisch, M. Steinbauer, M. Toeltsch, E. Bonek, and R. Thoma, "Capacity of MIMO systems based on measured wireless channels," *IEEE J. Selected Areas Comm.*, April 2002.

[32] M. Abramowitz and I. A. Stegun, *Handbook of Mathematical Functions*. New York, Dover, 1965.

[33] I. S. Gradshteyn and I. M. Ryzhik, *Table of Integrals, Series, and Products*. Academic Press, 1994.

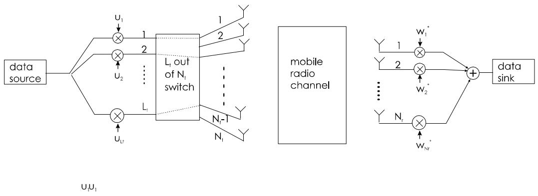

Fig. 1. System model

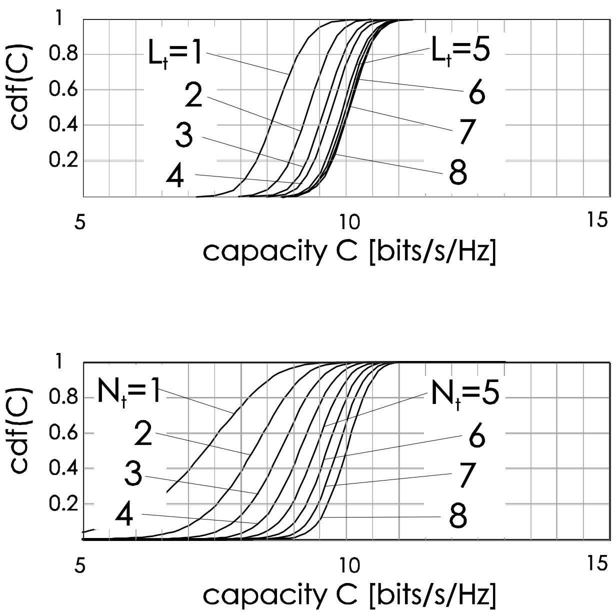

Fig. 2. Upper figure: Capacity of a system with H-S/MRT at the transmitter and MRC at the receiver for various values of L_t with $N_\mathrm{t} = 8$, $N_\mathrm{r} = 2$, $SNR = 20$ dB. Lower figure: capacity of a system with MRT at transmitter and MRC at receiver for various values of N_t and $N_\mathrm{r} = 2$, $SNR = 20$ dB.

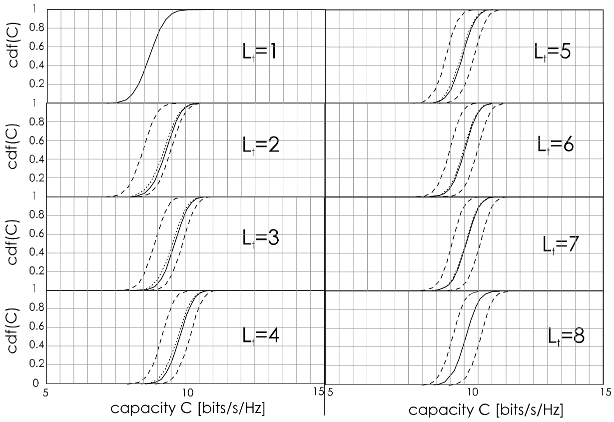

Fig. 3. Cdf of the capacity: lower bound (left dashed curves), upper bound (right dashed curves), exact (solid curves), and exact with the use of the simplified selection criterion (dotted). $N_\mathrm{t} = 8$, $N_\mathrm{r} = 8$, $SNR = 20dB$.

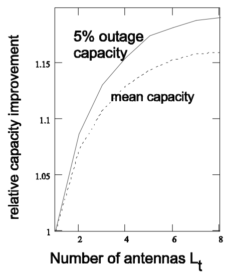

Fig. 4. Capacity increase of the 5% outage capacity and the ergodic capacity compared to $L_\mathrm{t} = 1$ when having several $active$ antennas at the transmitter. $N_\mathrm{t} = 8$, $N_\mathrm{r} = 2$, $SNR = 20dB$.

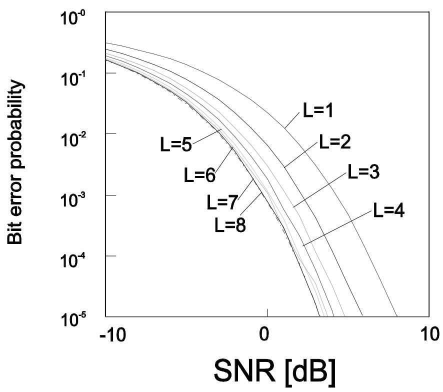

Fig. 5. BEP as a function of SNR for $\pi/4$-DQPSK as modulation format

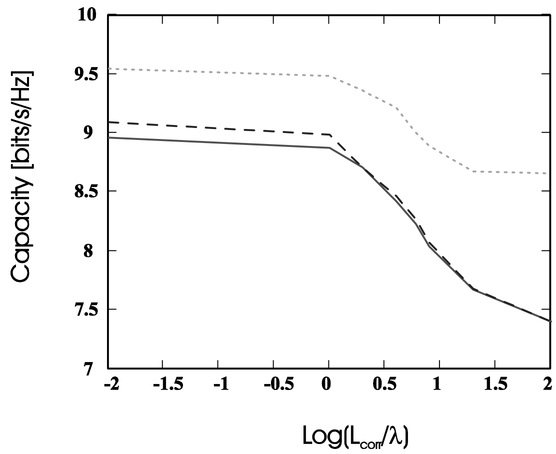

Fig. 6. 10% outage capacity of a system with 2 receiver antennas and H-S/MRT at the transmitter as a function of the antenna spacing. 3/8 system with optimum antenna selection (dashed), 3/8 system with antenna selection based on received power (solid) and 8/8 system (dotted). Correlation coefficient between signals at two antenna elements that are spaced d apart is $\exp(-d/L_{\mathrm{corr}})$.

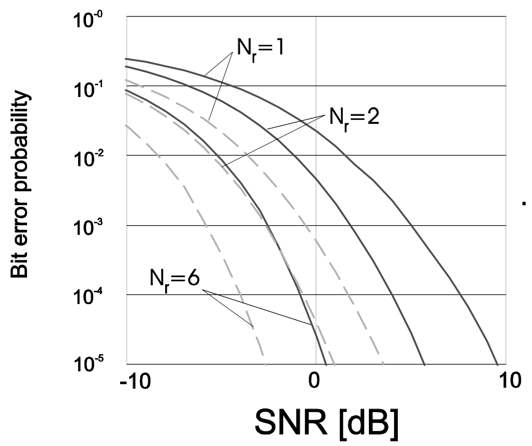

Fig. 7. Influence of the number of receive antennas on the BEP. MSK modulation; $8/8$ (solid) and $1/8$ (dashed) H-S/MRT at transmitter.

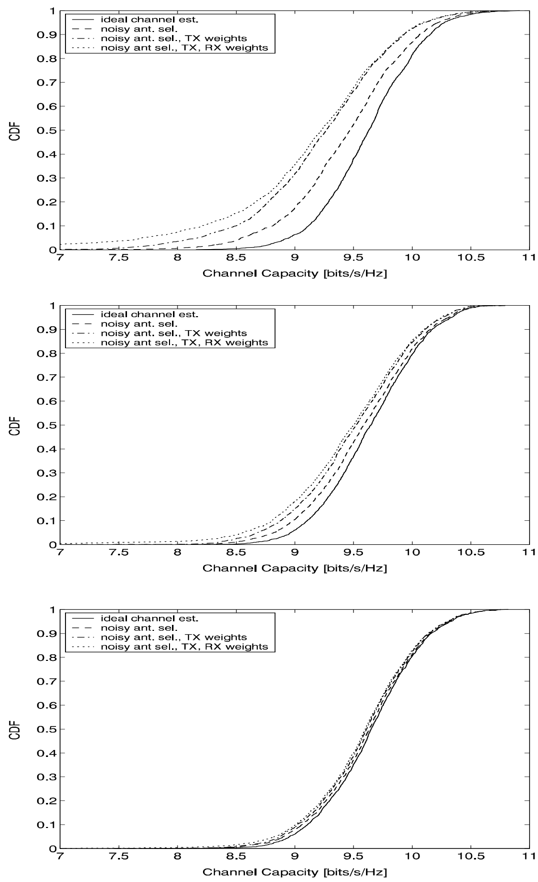

Fig. 8. Impact of errors in the estimation of transfer function matrix H. Cdf of the capacity for (i) ideal channel knowledge at TX and RX (solid), (ii) imperfect antenna selection, but perfect antenna weights (dashed), (iii) imperfect antenna weights at TX only (dotted), and (iv) imperfect antenna weights at TX and RX (dash-dotted). Top plot: $SNR_{\text{pilot}} = 5$ dB, middle plot: $SNR_{\text{pilot}} = 10$ dB, bottom plot $SNR_{\text{pilot}} = 15$ dB.

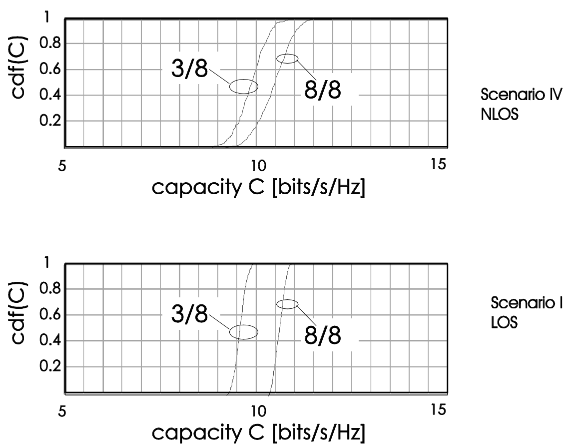

Fig. 9. Capacity of H-S/MRT system with $L_{\rm t} = 3$ and $N_{\rm t} = 8$ elements, and a MRT system with $N_{\rm t} = 8$ elements in a microcellular environment. See text for description of the scenarios.